Interaction Notes

Note 543

30 June 1998

AFRL/DEOB-PA
14 AUG 98

Application of Symmetry to Magnetic-Singularity Identification of Buried Targets

Carl E. Baum

Air Force Research Laboratory
Directed Energy Directorate

Abstract

A common class of buried targets has C_N symmetry (N-fold rotation axis) for $N \geq 3$. This makes the magnetic-polarizability dyadic decompose into longitudinal and transverse parts, each with its own natural frequencies (pure exponential decays in time for magnetic-singularity identification characterized by diffusion in metal). With appropriate three-axis coils (transmit and receive) above the ground surface, one can make measurements, which can be used to locate and orient (modulo sign on rotation axis) the target. This involves maving the coils above the ground and orienting the coils so as to find certain nulls in the data. A procedure (algorithm) is developed for this purpose.

Interaction Notes

Note 543

30 June 1998

Application of Symmetry to Magnetic-Singularity Identification of Buried Targets

Carl E. Baum

Air Force Research Laboratory
Directed Energy Directorate

Abstract

A common class of buried targets has C_N symmetry (N-fold rotation axis) for $N \geq 3$. This makes the magnetic-polarizability dyadic decompose into longitudinal and transverse parts, each with its own natural frequencies (pure exponential decays in time for magnetic-singularity identification characterized by diffusion in metal). With appropriate three-axis coils (transmit and receive) above the ground surface, one can make measurements, which can be used to locate and orient (modulo sign on rotation axis) the target. This involves moving the coils above the ground and orienting the coils so as to find certain nulls in the data. A procedure (algorithm) is developed for this purpose.

1. Introduction

In a previous paper [5] general considerations of symmetry were applied to the identification of buried targets. Both magnetic singularity identification (MSI) and electromagnetic singularity identification (EMSI) were considered.

For EMSI, which is applicable to both metal and dielectric targets (with typical frequencies in the 100 MHz to GHz regime), a significant identification signature has been pursued involving the lack of the hv (cross-pol) component of the backscattering dyadic (in the usual h,v radar coordinate system) for targets with O_2 or $C_{\infty a}$ symmetry (body of revolution (BOR) with axial symmetry planes) provided the rotation axis is perpenicular to the ground surface. Measurements using synthetic-aperture radar (SAR) have been made [8] and measures (norms) of cross polarization have been introduced [6].

For MSI, which is applicable to metal targets (with typical frequencies from below 100 Hz into the kHz range), symmetry introduces important simplifications in the magnetic-polarizability dyadic [3, 5, 11]. These can be exploited in target location and identification, and this is the subject of the present paper.

After reviewing the role of symmetry in the magnetic-polarizability dyadic, we go on to consider the use of symmetrical coils (loops) in transmission and reception for detecting symmetry in the target. Then we go on to consider techniques for locating such targets and determining their orientations.

2. Symmetry in Magnetic-Singularity Identification

Summarizing from [2-5, 11] the magnetic polarizability dyadic takes the form

$$\begin{aligned}
\overleftrightarrow{M}(s) &= \overleftrightarrow{M}(\infty) + \sum_{\alpha} M_{\alpha} \overrightarrow{M}_{\alpha} \overrightarrow{M}_{\alpha} [s - s_{\alpha}]^{-1} \\
&= \overleftrightarrow{M}(0) + s \sum_{\alpha} \frac{M_{\alpha}}{s_{\alpha}} \overrightarrow{M}_{\alpha} \overrightarrow{M}_{\alpha} [s - s_{\alpha}]^{-1} \\
\overrightarrow{M}(t) &= \overleftrightarrow{M}(\infty) \ \delta(t) + \sum_{\alpha} M_{\alpha} \overrightarrow{M}_{\alpha} \overrightarrow{M}_{\alpha} e^{s_{\alpha} t} u(t) \\
&= \overleftrightarrow{M}(0) \, \delta(t) + \sum_{\alpha} M_{\alpha} \overrightarrow{M}_{\alpha} \overrightarrow{M}_{\alpha} \left[\frac{\delta(t)}{s_{\alpha}} + e^{s_{\alpha} t} \ u(t) \right]^{-1}
\end{aligned} \tag{2.1}$$

appropriate for delta-function response. For step-function response this is

$$\begin{aligned}
\frac{1}{s} \overleftrightarrow{M}(s) &= \frac{1}{s} \overleftrightarrow{M}(0) + \sum_{\alpha} \frac{M_{\alpha}}{s_{\alpha}} \overrightarrow{M}_{\alpha} \overrightarrow{M}_{\alpha} [s - s_{\alpha}]^{-1} \\
\int_{-\infty}^{t} \overleftrightarrow{M}(t') \, dt' &= \left[\overleftrightarrow{M}(0) + \sum_{\alpha} \frac{M_{\alpha}}{s_{\alpha}} \overrightarrow{M}_{\alpha} \overrightarrow{M}_{\alpha} [s - s_{\alpha}]^{-1} \right] u(t)
\end{aligned} \tag{2.2}$$

where the presence of $\overleftrightarrow{M}(0)$ *(DC response) indicates the presence of a permeable target (e.g., iron), this itself being* a target discriminant. The various terms have the properties

$$\begin{aligned}
&\overrightarrow{M}_{\alpha} \cdot \overrightarrow{M}_{\alpha} = 1 \ , \ \overrightarrow{M}_{\alpha} \equiv \text{ real unit vector for } \alpha\text{th mode} \\
&M_{\alpha} \equiv \text{real scalar, } s_{\alpha} < 0 \ \text{(all negative real natural frequencies)} \\
&\overleftrightarrow{M}(\infty) = \sum_{\nu=1}^{3} M_{\nu}^{(\infty)} \overrightarrow{M}_{\nu}^{(\infty)} \overrightarrow{M}_{\nu}^{(\infty)} \\
&\overrightarrow{M}_{\nu_1}^{(\infty)} \cdot \overrightarrow{M}_{\nu_2}^{(\infty)} = 1_{\nu_1,\nu_1} \ \text{(orthonormal)} \ , \ \overrightarrow{M}_{\nu}^{(\infty)} \equiv \text{ real eigenvectors (three)} \\
&\overrightarrow{M}_{\nu}^{(\infty)} \equiv \text{ real eigenvalues (non positive, not necessarily distinct)}
\end{aligned} \tag{2.3}$$

$$\overset{\leftrightarrow}{M}(0) = \sum_{\nu=1}^{3} M_\nu^{(0)} \; \vec{M}_\nu^{(0)} \; M_\nu^{(0)} \tag{2.3}$$

$\vec{M}_{\nu_1}^{(0)} \cdot \vec{M}_{\nu_2}^{(0)} = 1_{\nu_1,\nu_2}$ (orthonormal) , $\vec{M}_\nu^{(0)} \equiv$ real eigenvectors (three)

$M_\nu^{(0)} \equiv$ real eigenvalues (non negative, not necessarily distinct) .

$$1_{\nu_1,\nu_2} = \begin{cases} 1 \text{ for } \nu_1 = \nu_2 \\ 0 \text{ for } \nu_1 \neq \nu_2 \end{cases}$$

$s = \Omega + j\omega \equiv$ complex frequency or two-sided Laplace-transform variable

In deriving these formulae the target is assumed linear and reciprocal. The external medium has no significant influence provided its permeability μ is the same as μ_0. Furthermore transit times in the external medium across the target and from target to transmitter and receiver (loops) are assumed small compared to decay times $\left(-s_\alpha{}^{-1}\right)$ of interest due to diffusion in the target. This also allows for the simple form of a constant $\overset{\leftrightarrow}{M}(\infty)$ for the SEM entire function, this being the magnetic-polarizability dyadic of a perfectly conducting target of the same shape [2].

Table 2.1 from [3] summarizes the implications of symmetry for the magnetic polarizability dyadic. For finite-dimensioned targets it is the point symmetry groups (involving transformations which leave $|\vec{r}_1 - \vec{r}_2|$ invariant for all $\vec{r}_1$ and $\vec{r}_2$ positions on the target) which are of interest [10]. Since we are considering only the induced magnetic-dipole moment (magnetic-quadrupole and higher-order moments being neglected in the MSI approximations), the possible types of dyadics simplify considerably. The various unit vectors $\vec{M}_\alpha$ align according to the various symmetry planes and axes, so that they line up as

$$\vec{M}_{\alpha_1} \cdot \vec{M}_{\alpha_2} = \begin{cases} \pm 1 & \text{(parallel or antiparallel)} \\ 0 & \text{(perpendicular)} \end{cases} \tag{2.4}$$

where we note the sign ambiguity on each $\vec{M}_\alpha$ which can equally well be replaced by $-\vec{M}_\alpha$ in the dyadic representation. In an appropriate Cartesian reference each can be represented by only one of the unit vectors as

$$\vec{M}_\alpha = \vec{1}_y \text{ or } \vec{1}_y \text{ or } \vec{1}_z \tag{2.5}$$

In following sections, we assume that the target has certain of the symmetries in the table. As we shall see, the second entry (from $C_{2\alpha}$ or D_2 symmetry) can be distinguished from the third (higher order rotation/reflection).

This third category, where the polarizability dyadic splits into a longitudinal ($\vec{1}_z\vec{1}_z$) and a transverse ($\overleftrightarrow{1}_z$) part, has a two-fold degeneracy in the transverse part and is readily distinguishable from the second category. It is interesting to note that, since we are dealing with only the magnetic-dipole part of the scattering, we do not need $C_{\infty a}$ symmetry (as in the case of EMSI where wavelengths in the external medium are of the order of the target dimensions). For example, a three-fold (or higher) rotation axis is sufficient to obtain this transverse polarization independence. This is convenient because C_{Na} symmetry (N-fold axis for various N with axial symmetry planes) models many types of mines and unexploded ordnance (shells, rockets, etc.). The fourth category in the table has triple degeneracy, but is not commonly employed for mines and UXO.

Table 2.1. Decomposition of Magnetic Polarizability Dyadic According to Target Point Symmetries.

Form of $\overleftrightarrow{\tilde{M}}(s)$	Symmetry Types (Groups)	Symmetry Category
$\tilde{M}_z(s)\,\vec{1}_z\vec{1}_z + \overleftrightarrow{\tilde{M}}_t(s)$ $(\overleftrightarrow{\tilde{M}}_t(s)\cdot\vec{1}_z = \vec{0})$	R_z (single symmetry plane) C_2 (2-fold rotation axis)	1
$\tilde{M}_z(s)\,\vec{1}_z\vec{1}_z + \tilde{M}_x(s)\,\vec{1}_x\vec{1}_x + \tilde{M}_y(s)\,\vec{1}_y\vec{1}_y$	$C_{2a} = R_x \otimes R_y$(two axial symmetry planes) D_2 (three 2–fold rotation axes)	2
$\tilde{M}_z(s)\,\vec{1}_z\vec{1}_z + \tilde{M}_t(s)\,\overleftrightarrow{1}_z$ $\left(\overleftrightarrow{1}_z = \overleftrightarrow{1} - \vec{1}_z\vec{1}_z \Rightarrow \text{double degeneracy}\right)$	C_N for $N \geq 3$ (N - fold rotation axis) S_N for N even and $N \geq 4$ (N - fold rotation - reflection axis) D_{2d} (three 2 - fold rotation axes plus diagonal symmetry planes)	3
$\tilde{M}(s)\,\overleftrightarrow{1}$ $\left(\overleftrightarrow{1} \Rightarrow \text{triple degeneracy}\right)$	O_3 (generalized sphere) T, O, Y (regular polyhedra)	4

3. Measurement Coordinates

With the target at $\vec{r}_0$ (which we can take as $\vec{0}$ for convenience) and the transmitter and receiver (sensor) both at $\vec{r}_s$ we have

$$R = |\vec{r}_s - \vec{r}_0| \, , \quad \vec{1}_R = \frac{\vec{r}_s - \vec{r}_0}{R} \tag{3.1}$$

Then with the transmitter loop approximated as a magnetic dipole we have at the target (quasi-static, near-field approximation)

$$\begin{aligned}
\tilde{\vec{H}}^{(inc)}(s) &= \frac{1}{4\pi R^3}\left[3\,\vec{1}_R\,\vec{1}_R - \overleftrightarrow{1}\right]\cdot\tilde{\vec{m}}^{(inc)}(s) \\
\tilde{\vec{m}}^{(inc)}(s) &= \tilde{m}^{(inc)}(s)\;\vec{1}_c \\
\vec{1}_c &\equiv \text{orientation of transmitter coil} \\
\overleftrightarrow{1} &= \vec{1}_x\vec{1}_x + \vec{1}_y\vec{1}_y + \vec{1}_z\vec{1}_z \equiv \text{identity dyadic}
\end{aligned} \tag{3.2}$$

Then the scattering has [2, 11]

$$\begin{aligned}
\tilde{\vec{m}}^{(sc)}(s) &= \tilde{\overleftrightarrow{M}}(s)\cdot\tilde{\vec{H}}^{(inc)}(s) \\
\tilde{\vec{H}}^{(sc)}(s) &= \frac{1}{4\pi R^3}\left[3\,\vec{1}_R\,\vec{1}_R - \overleftrightarrow{1}\right]\cdot\tilde{\vec{m}}^{(sc)}(s)
\end{aligned} \tag{3.3}$$

With the scattered field being measured at the receiver in the direction $\vec{1}_s$, we have a signal proportional to

$$\begin{aligned}
\tilde{H}^{(sc)}(s) &= \vec{1}_s\cdot\tilde{\overleftrightarrow{H}}^{(sc)}(s) = \frac{1}{4\pi R^3}\,\vec{1}_s\cdot\left[3\,\vec{1}_R\,\vec{1}_R - \overleftrightarrow{1}\right]\cdot\tilde{\vec{m}}^{(sc)}(s) \\
&= \frac{1}{16\pi^2 R^6}\,\vec{1}_s\cdot\left[3\,\vec{1}_R\,\vec{1}_R - \overleftrightarrow{1}\right]\cdot\tilde{\overleftrightarrow{M}}(s)\cdot\left[3\,\vec{1}_R\,\vec{1}_R - \overleftrightarrow{1}\right]\cdot\tilde{\vec{m}}^{(inc)}(s) \\
&= \frac{\tilde{m}^{(inc)}(s)}{16\pi^2 R^6}\,\vec{1}_s\cdot\left[3\,\vec{1}_R\,\vec{1}_R - \overleftrightarrow{1}\right]\cdot\tilde{\overleftrightarrow{M}}(s)\cdot\left[3\,\vec{1}_R\,\vec{1}_R - \overleftrightarrow{1}\right]\cdot\vec{1}_c
\end{aligned} \tag{3.4}$$

This suggests that we define a normalized transfer function as

$$\tilde{T}(s) \equiv \vec{1}_s \cdot \left[3\, \vec{1}_R \vec{1}_R - \overleftrightarrow{1} \right] \cdot \overleftrightarrow{\tilde{M}}(s) \cdot \left[3\, \vec{1}_R \vec{1}_R - \overleftrightarrow{1} \right] \cdot \vec{1}_c$$
$$\tilde{H}_s(s) = \frac{\tilde{m}^{(inc)}}{16\pi^2 R^6}\, \tilde{T}(s) \qquad (3.5)$$

containing the frequency and aspect-dependent information of the target.

Figure 3.1 shows the general location of a buried target with a symmetry axis $\vec{1}_a$ corresponding to the category 3 symmetry discussed previously which we can generally refer to as rotational. For convenience we define Cartesian (x, y, z) and cylindrical (Ψ, ϕ, z) coordinates centered on $\vec{r}_0$ with

$$\vec{1}_z = \vec{1}_a$$
$$x = \Psi\cos(\phi) \quad , \quad y = \Psi\sin(\phi) \qquad (3.6)$$

and the x axis ($\phi = 0$) is chosen as parallel to the ground surface. Above the ground we have primed coordinates with $\vec{1}_{z'}$ now taken as vertical (perpendicular to ground surface). The coordinates are centered at some height h above the surface. Since we do not necessarily know the target location a priori, the x' axis is not in general parallel to the x axis, but later we consider how to locate the x axis and thereby bring these into alignment. We would also like to be able to move the sensor location to be located on the z axis to take full advantage of the symmetry.

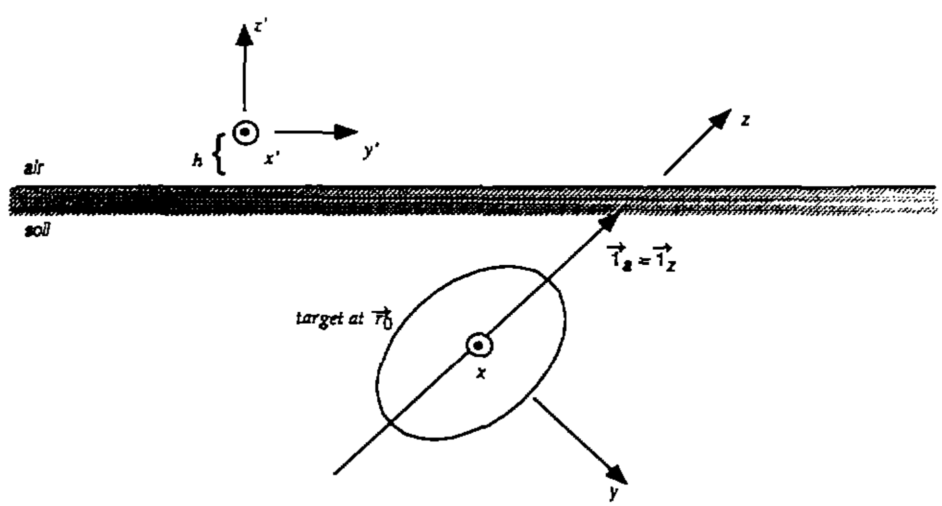

Fig. 3.1 Measurement Coordinates

4. Cross-Pol Symmetry Detector

Before going on to the general case, let us consider a simpler case where we assume that

$$\begin{aligned} &\vec{1}_z = \vec{1}_{z'} \quad \text{(vertical target)} \\ &x' = x \ , \quad y' = y \quad \text{(transmitter / receiver directly above target)} \\ &\vec{1}_r = \vec{1}_z \end{aligned} \tag{4.1}$$

Then we have, assuming the third symmetry category,

$$\begin{aligned} \tilde{T}(s) &= \vec{1}_s \cdot \left[2\ \vec{1}_z \vec{1}_z - \overleftrightarrow{1}_z \right] \cdot \left[\tilde{M}_z(s) \vec{1}_z \vec{1}_z + \tilde{M}_t(s) \overleftrightarrow{1}_z \right] \\ &\quad \cdot \left[2\ \vec{1}_z \vec{1}_z - \overleftrightarrow{1}_z \right] \cdot \vec{1}_c \\ &= 4\ \vec{1}_s \cdot \vec{1}_z \vec{1}_z \cdot \vec{1}_m\ \tilde{M}_z(s) + \vec{1}_s \cdot \overleftrightarrow{1}_z \cdot \vec{1}_m\ \tilde{M}_t(s) \end{aligned} \tag{4.2}$$

so that the longitudinal and transverse parts neatly separate.

Choosing, as a first case,

$$\vec{1}_c = \vec{1}_z \tag{4.3}$$

we have

$$\tilde{T}(s) = 4\ \vec{1}_s \cdot \vec{1}_z\ \tilde{M}_z(s) \tag{4.4}$$

so that for $\vec{1}_s$ perpendicular to $\vec{1}_z$ we have

$$\tilde{T}(s) = 0 \tag{4.5}$$

this being the case as $\vec{1}_s$ is rotated about the z axis. Of course, by reciprocity, one can choose $\vec{1}_m$ for the transmitter perpendicular to $\vec{1}_z$ and rotate $\vec{1}_m$ to observe a null response for $\vec{1}_s$ in the z direction. Note that this signature applies to category two and one symmetries as well due to the decoupling of longitudinal and transverse scattering.

Choosing, as a second case,

$$\vec{1}_c = \vec{1}_x \ , \ \ \vec{1}_s = \vec{1}_{y'} \tag{4.6}$$

from (4.2) we again have for the third symmetry category

$$\tilde{T}(s) = 0 \tag{4.7}$$

However, as we rotate $\vec{1}_{x'}$ around the z axis ($\vec{1}_{y'}$ remaining perpendicular to $\vec{1}_{x'}$) then for the second symmetry category we have a non-null response for $\vec{1}_{x'}$ *not* aligned parallel (or antiparallel) to the x or y axes of the target. A non-null response in such an experiment also applies to the first symmetry category. Between these two cases we have a discriminant between the third and lower symmetry categories.

One can design a set of three loops which do not couple to each other by appropriate symmetry. For example, each loop can lie in a separate plane of three mutually perpendicular planes with the other two planes as symmetry planes of each loop. One can also have the loops have a common center so as to maintain a common distance from the target. The loop structure can itself have the third symmetry category with respect to the z axis. One can even have three identical loops at right angles with octahedral (O) symmetry, each loop utilizing four edges of the octahedron. An example of such symmetry is the O3L (octahedral 3-axis loop) used for magnetic-field measurements [9].

5. Co-Pol Symmetry Detector

Now generalize Section 4 by allowing $\vec{1}_m$ and $\vec{1}_s$ to assume all combinations of $\vec{1}_{x'}$, $\vec{1}_{y'}$, and $\vec{1}_{z'}$, giving a full three-axis transmitter/receiver. In this case one can measure the full magnetic-polarizability dyadic, noting the common R in (3.4) for all the measurements. If one does not know R, then one obtains some scalar constant times $\overleftrightarrow{\tilde{M}}(s)$. The longitudinal/transverse decomposition as in (4.2) still applies for category 3 symmetry. For lower order symmetry the transverse part is not in general diagonal but has mixed x', y' components.

By measuring the 3 x 3 dyadic (factoring out the transmitter strength and receiver sensitivity) we have

$$\overleftrightarrow{\tilde{X}}(s) = \frac{1}{16\pi^2 R^6}\left[2\,\vec{1}_z\vec{1}_z - \overleftrightarrow{1}_z\right]\cdot\left[\tilde{M}_z(s)\,\vec{1}_z\vec{1}_z + \overleftrightarrow{\tilde{M}}_t(s)\right] \cdot\left[2\,\vec{1}_z\vec{1}_z - \overleftrightarrow{1}_z\right] \tag{5.1}$$

appropriate to category one and higher symmetry. Noting that

$$\left[2\,\vec{1}_z\vec{1}_z - \overleftrightarrow{1}_z\right]^{-1} = \frac{1}{2}\vec{1}_z\vec{1}_z - \overleftrightarrow{1}_z \tag{5.2}$$

we can transform the measurements as

$$\begin{aligned}\overleftrightarrow{\tilde{X}}'(s) &= \left[\frac{1}{2}\vec{1}_z\vec{1}_z - \overleftrightarrow{1}_z\right]\cdot\overleftrightarrow{\tilde{X}}(s)\left[\frac{1}{2}\vec{1}_z\vec{1}_z - \overleftrightarrow{1}_z\right] \\ &= \frac{1}{16\pi^2 R^6}\left[\tilde{M}_z(s)\,\vec{1}_z\vec{1}_z + \overleftrightarrow{\tilde{M}}_t(s)\right]\end{aligned} \tag{5.3}$$

which neatly exhibits the magnetic polarizability tensor times a distance-scaling scalar. This type of "deconvolution" actually requires no particular symmetry in the target, just that the transmitter/receiver lie directly above the target (or more generally have the z' axis through the target, i.e., non vertical, and use the z' direction instead of the z direction (vertical) in the above.

With the longitudinal and transverse parts separated one can explore the properties of $\overleftrightarrow{M}_t(s)$ by diagonalizing it. If it can be diagonalized with real, frequency-independent unit eigenvectors then the symmetry is category 2 or higher. If the two eigenvalues are the same for all frequencies, then the orientation of the eigenvactors is not unique due to the two-fold degeneracy, implying category 3 symmetry.

This requires the design of coils for the three-axis measurement including both transmit and receive. Here symmetry can be used to minimize the coupling of one transmitter coil (e.g., x') to the other two (y' and z'). this is the same problem as in Section 4 and the same use of three symmetry planes is applicable. However, the transmit and receive coils in the same plane (e.g., x' = 0) need to have minimum coupling to each other while still maintaining the previous symmetry to minimize coupling to coils on other planes. One way to do this is to use three circular coaxial coils, two for transmit and one for receive [7], or conversely by reciprocity. Variations on this scheme for selection of coil radii and numbers of turns are possible and need to be explored. An alternate approach uses two coplanar coils, one each for transmit and receive, with the conductors crossing each other (perhaps at right angles) with due care near the crossing position so that the mutual inductance between them is zero. Calculations for a two-dimensional pair of such coils have been performed in [1 (Section 4)]. A variety of planar coil shapes (elliptical, triangular, etc.) are possible. Figure 5.1 shows an example of three such coplanar coil pairs on three orthogonal symmetry planes. Higher order symmetries can also be incorporated.

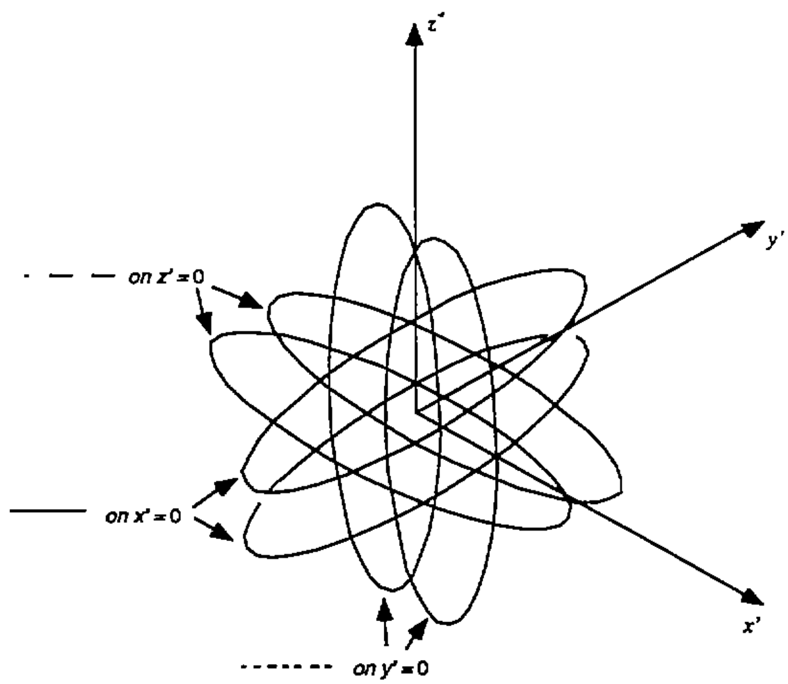

Fig. 5.1 Three Non-Coupling Loop Pairs on Three Orthogonal Symmetry Planes

6. Location and Identification of Symmetric Targets

Assume that the target of interest has category 3 symmetry so that $\overleftrightarrow{\tilde{M}}_t(s)$ is doubly degenerate. Now also let the target be buried with some unknown position and orientation (as might be appropriate for certain types of UXO). So the origin $\vec{r}_0$ and the orientations of the (x, y, z) coordinates are assumed unknown. However, the symmetry makes only $\vec{1}_z$ as the relevant orientation due to the degeneracy vis-à-vis $\vec{1}_x$ and $\vec{1}_y$. For convenience, one can then take $\vec{1}_x$ as horizontal (parallel to the ground surface).

The sensors are located at $\vec{r}_s$ and use the (x', y', z') coordinates. $\vec{1}_{z'}$ is specified as vertical, but x' and y' can be chosen arbitrarily parallel to the ground surface (horizontal), but mutually perpendicular. By moving the sensors parallel to the ground surface and rotating them we would like to be able to locate and discover the orientation $\vec{1}_z$ of the target (within the sign ambiguity on the direction of the z axis).

With some initial choice of $\vec{r}_s$ and the horizontal direction $\vec{1}_{x'}$ ($\vec{1}_{z'}$ being vertical), successive measurements with $\vec{1}_c$ and $\vec{1}_s$ taken as all choices of $\vec{1}_{x'}$, $\vec{1}_{y'}$ and $\vec{1}_{z'}$ defines a 3 X 3 dyadic

$$
\begin{aligned}
\tilde{X}_{n,m}(s) &= \frac{1}{16\pi^2 R^6}\,\vec{1}_n \cdot \left[3\,\vec{1}_R\vec{1}_R - \overleftrightarrow{1}\right] \cdot \overleftrightarrow{\tilde{M}}(s) \\
&\qquad \cdot \left[3\,\vec{1}_R\vec{1}_R - \overleftrightarrow{1}\right] \cdot \vec{1}_m \\
&= \frac{1}{16\pi^2 R^6}\,\vec{1}_n \cdot \left[3\,\vec{1}_R\vec{1}_R - \overleftrightarrow{1}\right] \cdot \left[\tilde{M}_z(s)\,\vec{1}_z\vec{1}_z + \tilde{M}_t(s)\,\overleftrightarrow{1}_z\right] \\
&\qquad \cdot \left[3\,\vec{1}_R\vec{1}_R - \overleftrightarrow{1}\right] \cdot \vec{1}_m \\
\overleftrightarrow{\tilde{X}}(s) &= \frac{1}{16\pi^2 R^6}\left[3\,\vec{1}_R\vec{1}_R - \overleftrightarrow{1}\right] \cdot \left[\tilde{M}_z(s)\,\vec{1}_z\vec{1}_z + \tilde{M}_t(s)\,\overleftrightarrow{1}_z\right] \\
&\qquad \cdot \left[3\,\vec{1}_R\vec{1}_R - \overleftrightarrow{1}\right] \\
&= \overleftrightarrow{\tilde{X}}^{(z)}(s) + \overleftrightarrow{\tilde{X}}^{(t)}(s) \\
\overleftrightarrow{\tilde{X}}^{(z)}(s) &= \frac{\tilde{M}_z(s)}{16\pi^2 R^6}\,\overrightarrow{\Theta}^{(z)} \\
\overleftrightarrow{\tilde{X}}^{(t)}(s) &= \frac{\tilde{M}_t(s)}{16\pi^2 R^6}\,\overrightarrow{\Theta}^{(t)}
\end{aligned}
$$

$$
\begin{aligned}
\overleftrightarrow{\Theta}^{(z)} &= \left[3\,\vec{1}_R\vec{1}_R - \overleftrightarrow{1}\right]\cdot\vec{1}_z\vec{1}_z\cdot\left[3\,\vec{1}_R\vec{1}_R - \overleftrightarrow{1}\right] \\
&= \left[3\left[\vec{1}_R\cdot\vec{1}_z\right]\vec{1}_R - \vec{1}_z\right]\left[3\left[\vec{1}_R\cdot\vec{1}_z\right]\vec{1}_R - \vec{1}_z\right] \\
&= 9\left[\vec{1}_R\cdot\vec{1}_z\right]^2\vec{1}_R\vec{1}_R - 3\left[\vec{1}_R\cdot\vec{1}_z\right]\left[\vec{1}_R\vec{1}_z + \vec{1}_z\vec{1}_R\right] + \vec{1}_z\vec{1}_z \\
\overleftrightarrow{\Theta}^{(t)} &= \left[3\,\vec{1}_R\vec{1}_R - \overleftrightarrow{1}\right]\cdot\overleftrightarrow{1}_z\cdot\left[3\,\vec{1}_R\vec{1}_R - \overleftrightarrow{1}\right] \\
&= 9\left[\vec{1}_R\cdot\overleftrightarrow{1}_z\cdot\vec{1}_R\right]\vec{1}_R\vec{1}_R - 3\left[\vec{1}_R\vec{1}_R\cdot\overleftrightarrow{1}_z + \overleftrightarrow{1}_z\cdot\vec{1}_R\vec{1}_R\right] + \overleftrightarrow{1}_z \\
&= \left[3\,\vec{1}_R\vec{1}_R - \overleftrightarrow{1}\right]^2 - \overleftrightarrow{\Theta}^{(z)} \quad \left(\text{from } \overleftrightarrow{1}_z = \overleftrightarrow{1} - \vec{1}_z\vec{1}_z\right)
\end{aligned}
\tag{6.1}
$$

Diagonalizing $\tilde{\overleftrightarrow{X}}(s)$ will, in general, not directly exhibit $\vec{1}_z$ or $\vec{1}_R$ due to the mixing of the longitudinal and transverse parts with the different frequency dependences of $\tilde{M}_z(s)$ and $\tilde{M}_t(s)$.

Note that if $\tilde{M}_z(s) = \tilde{M}_t(s)$, we have the case of category 4 symmetry in which $\tilde{\overleftrightarrow{X}}(s)$ is readily diagonalizable, giving eigenvectors as $\pm\,\vec{1}_R$ (giving direction to the target) and two vectors perpendicular to $\vec{1}_R$. Which is $\vec{1}_R$ is distinguished by the non-degenerate eigenvalue, the other two vectors having equal eigenvalues. In such a case we can choose $\vec{1}_z$ arbitrarily.

An alternate approach for category 3 symmetry involves recognition of the target by the natural frequencies s_{α_z} and s_{α_t} in

$$
\begin{aligned}
\tilde{M}_z(s) &= \tilde{M}_z(\infty) + \sum_{s_{\alpha_z}} M_{\alpha_z}\left[s - s_{\alpha_z}\right]^{-1} \\
\tilde{M}_t(s) &= \tilde{M}_t(\infty) + \sum_{s_{\alpha_t}} M_{\alpha_t}\left[s - s_{\alpha_t}\right]^{-1}
\end{aligned}
\tag{6.2}
$$

Having identified which kind of target is present, then construct any convenient parts of $\tilde{\overleftrightarrow{X}}^{(z)}(s)$ and $\tilde{\overleftrightarrow{X}}^{(t)}(s)$ (just one each large M_{α_z} and M_{α_t} may be sufficient). The important point is that one obtains angular functions that one can investigate for locating and orienting the target.

It is interesting to note special cases for the angular functions in (6.1). A first case has

$$
\begin{aligned}
&\vec{1}_R = \pm \vec{1}_z \qquad \text{(longitudinal observer)} \\
&\overleftrightarrow{\Theta}^{(z)} = 4\, \vec{1}_z \vec{1}_z \;, \quad \overleftrightarrow{\Theta}^{(t)} = \vec{1}_z
\end{aligned}
\tag{6.3}
$$

A second case has

$$
\begin{aligned}
&\vec{1}_R \cdot \vec{1}_z = 0 \;, \quad \overleftrightarrow{1}_z \cdot \vec{1}_R = \vec{1}_R \qquad \text{(transverse observer)} \\
&\quad \overleftrightarrow{\Theta}^{(z)} = \vec{1}_z \vec{1}_z \;, \quad \overleftrightarrow{\Theta}^{(t)} \;\; 3\, \vec{1}_R \vec{1}_R + \overleftrightarrow{1}_z
\end{aligned}
\tag{6.4}
$$

While these are simpler expressions, a remarkable relation between the two for both cases is

$$
\begin{aligned}
\overleftrightarrow{\Theta}^{(z)} \cdot \overleftrightarrow{\Theta}^{(t)} &= \times \overleftrightarrow{O} \quad \text{(all 9 components zero)} \\
&= \overleftrightarrow{\Theta}^{(t)} \cdot \overleftrightarrow{\Theta}^{(z)}
\end{aligned}
\tag{6.5}
$$

So a question arises as to whether such a zero dyadic can be used to determine whether such cases as above can be distinguished in an experiment. Note that (6.5) is equivalent to

$$
\overleftrightarrow{\tilde{X}}^{(z)}(s) \cdot \overleftrightarrow{\tilde{X}}^{(t)}(s) = \overleftrightarrow{O} = \overleftrightarrow{\tilde{X}}^{(t)}(s) \cdot \overleftrightarrow{\tilde{X}}^{(z)}(s)
\tag{6.6}
$$

in a frequency-independent manner.

So define

$$
\begin{aligned}
\overleftrightarrow{\Theta}^{(1)} &\equiv \overleftrightarrow{\Theta}^{(z)} \cdot \overleftrightarrow{\Theta}^{(t)} \\
&= \left[3\, \vec{1}_R \vec{1}_R - \overleftrightarrow{1}\right] \cdot \vec{1}_z \vec{1}_z \cdot \left[3\, \vec{1}_R \vec{1}_R - \overleftrightarrow{1}\right]^2 \cdot \overleftrightarrow{1}_z \cdot \left[3\, \vec{1}_R \vec{1}_R - \overleftrightarrow{1}\right]
\end{aligned}
\tag{6.7}
$$

Noting that we have an inverse

$$\left[3\,\vec{1}_R\,\vec{1}_R - \overleftrightarrow{1}\right]^{-1} = \frac{3}{2}\,\vec{1}_R\,\vec{1}_R - \overleftrightarrow{1} \tag{6.8}$$

we can dot multiply this on both sides of $\overleftrightarrow{\Theta}^{(1)}$, which is the zero dyadic iff

$$\overleftrightarrow{\Theta}^{(2)} \equiv \vec{1}_z\,\vec{1}_z \cdot \left[3\,\vec{1}_R\,\vec{1}_R - \overleftrightarrow{1}\right]^2 \cdot \overleftrightarrow{1}_z \tag{6.9}$$

is the zero dyadic. This is the zero dyadic iff the vector

$$\vec{\Theta}^{(3)} \equiv \vec{1}_z \cdot \left[3\,\vec{1}_R\,\vec{1}_R - \overleftrightarrow{1}\right]^2 \cdot \overleftrightarrow{1}_z \tag{6.10}$$

is the zero vector $\vec{0}$. Define a transverse vector $\vec{1}_t$ by

$$\vec{1}_t \cdot \vec{1}_z = 0 \tag{6.11}$$

which is then a linear combination of $\vec{1}_x$ and $\vec{1}_y$. Dot multiplying this with $\overleftrightarrow{\Theta}^{(3)}$ gives a scalar

$$\Theta^{(4)} \equiv \vec{1}_z \cdot \left[3\,\vec{1}_R\,\vec{1}_R - \overleftrightarrow{1}\right]^2 \cdot \vec{1}_t \tag{6.12}$$

Then $\vec{\Theta}^{(3)}$ is the zero vector iff $\Theta^{(4)}$ is zero for all possible $\vec{1}_t$. Note that no z component of the vector need be considered since it is annihilated by $\overleftrightarrow{1}_z$. Consider two linearly independent choices of $\vec{1}_t$. First we have

$$\vec{1}_t \cdot \vec{1}_R = 0 \quad \text{(perpendicular to } \vec{1}_R \text{ and } \vec{1}_z\text{)}$$

$$\begin{aligned} \overleftrightarrow{\Theta}^{(4)} &\equiv \vec{1}_z \cdot \left[3\,\vec{1}_R\,\vec{1}_R - \overleftrightarrow{1}\right] \cdot \left[3\,\vec{1}_R\,\vec{1}_R - \overleftrightarrow{1}\right] \cdot \vec{1}_t \\ &= \left[3\left[\vec{1}_R \cdot \vec{1}_z\right]\vec{1}_R - \vec{1}_z\right] \cdot \left[-\vec{1}_t\right] \\ &= 0 \end{aligned} \tag{6.13}$$

independent of $\vec{1}_R$. Second we have

$$\vec{1}_t \text{ in plane of } \vec{1}_R \text{ and } \vec{1}_z$$

$$\begin{aligned}\Theta^{(4)} &\equiv \vec{1}_z \cdot \left[3\,\vec{1}_R\vec{1}_R - \overleftrightarrow{1}\right] \cdot \left[3\,\vec{1}_R\vec{1}_R - \overleftrightarrow{1}\right] \cdot \vec{1}_t \\ &= \vec{1}_z \cdot \left[3\,\vec{1}_R\vec{1}_R + \overleftrightarrow{1}\right] \cdot \vec{1}_t \\ &= 3\left[\vec{1}_R \cdot \vec{1}_z\right]\left[\vec{1}_R \cdot \vec{1}_t\right]\end{aligned} \tag{6.14}$$

which is zero iff

$$\begin{aligned}&\vec{1}_R \cdot \vec{1}_t = 0 \Rightarrow \vec{1}_R = \pm\vec{1}_z \quad \text{(first case) or} \\ &\vec{1}_R \cdot \vec{1}_z = 0 \quad \text{(second case)}\end{aligned} \tag{6.15}$$

Therefore $\overleftrightarrow{\Theta}^{(1)}$ is the zero dyadic iff one of the two cases ((6.3) and (6.4)) applies.

So now we have a test from our data in (6.6) for whether we have positioned our sensor so that one of the two cases applies. Defining a norm

$$\tilde{N}(s) \equiv \left\| \tilde{\overleftrightarrow{X}}^{(z)}(s) \cdot \tilde{\overleftrightarrow{X}}^{(t)}(s) \right\| \tag{6.16}$$

in some convenient way (2-norm, root span, largest element magnitude, etc.) gives a scalar which is zero iff one of the two cases applies. Of source, real data has noise so some minimum is sought.

One form an experiment might take is as follows. Keep the sensor on the sensor plane (a constant height h above the ground). Case 1 has a straight line through the target parallel to $\pm\vec{1}_z$, intersecting the sensor plane in one point P_0 except in the special case that $\vec{1}_z$ is horizontal (perpendicular to $\vec{1}_{z'}$). (See fig. 6.1.) Case 2 has $\vec{1}_R$ perpendicular to and determining a plane (the target plane) passing through the target and perpendicular to $\vec{1}_z$. The target plane intersects the sensor plane in a straight line C (except in the special case that $\vec{1}_z = \vec{1}_{z'}$).

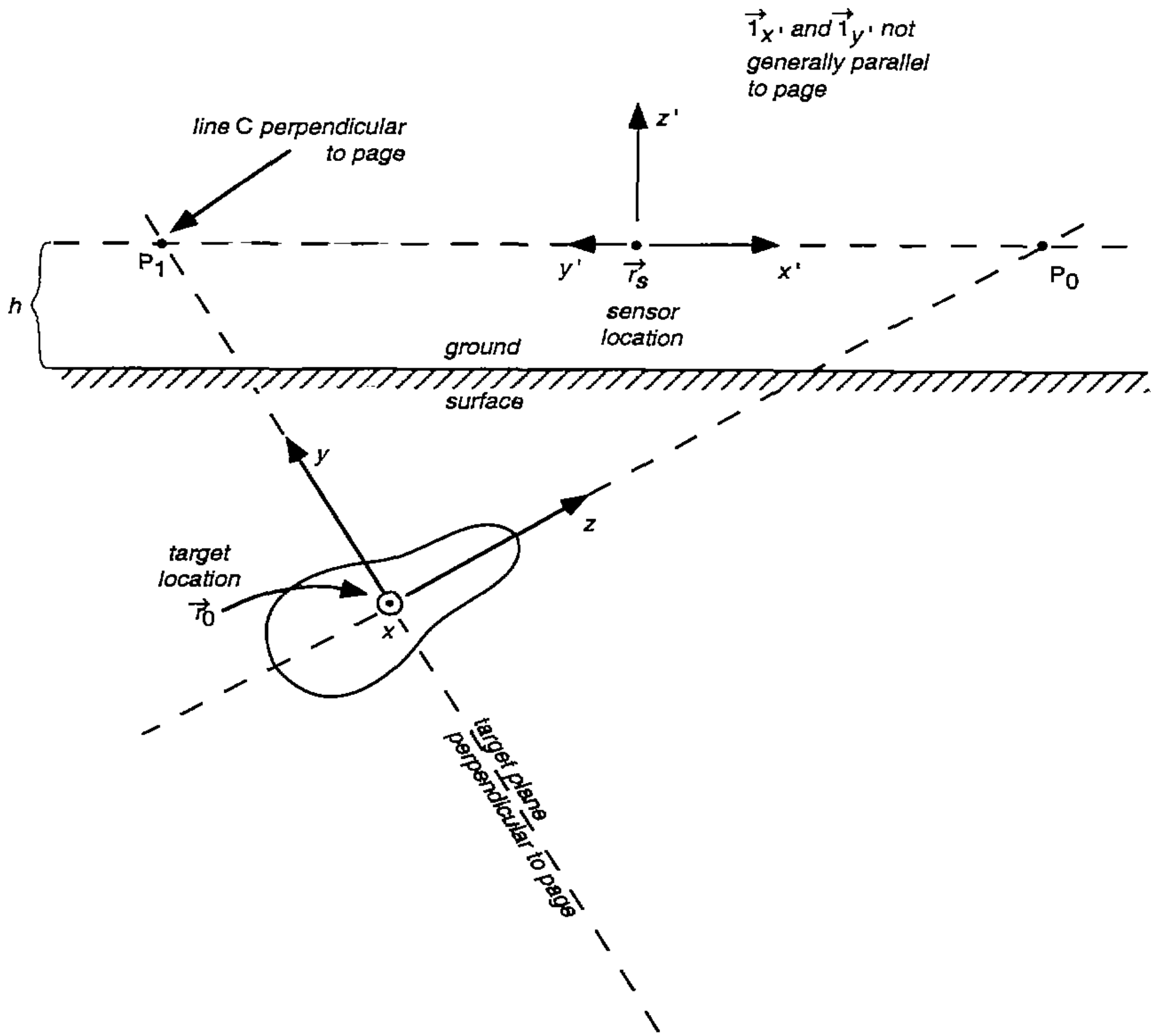

Fig. 6.1 Geometry for Target Location and Orientation

Referring to fig. 6.1, we have a side view containing the target axis. The target plane, sensor plane, and line C are parallel to our line of sight. In this view, the target coordinates fix our orientation. The sensor coordinates have z' up, but x' and y' (mutually orthogonal) are oriented at some unknown angle in the sensor plane.

So now move the sensor location in some straight line (reversing direction if necessary), keeping the height h fixed until our norm in (6.16) is nulled (not exactly zero due to noise). This finds a point on C (case 2, unless the path is parallel to C or passes through the point R_0). Next move along C, keeping $\tilde{N}(s)$ nulled; this determines the orientation of the x axis of the target. Now the sensors can be rotated about the z' axis so that x is parallel to x. move along C until one finds

$$\begin{aligned} \tilde{X}_{x',x'}(s) &= \tilde{X}_{x,x}(s) \text{ contains only } \tilde{M}_t(s)\left(\text{no } \tilde{M}_z(s)\right) \\ \tilde{X}_{n,m}(s) &= 0 \text{ for } (n,m) = \begin{cases} (x',y') \\ (x',z') \\ (y',x') \\ (z',y') \end{cases} \end{aligned} \tag{6.17}$$

At this location, which we can call R_1, the signal is partially split in that the transverse part is exhibited in $\tilde{X}_{x',x'}(s)$. The observer is now on a vertical plane passing through the target and containing the z and y axes. This is also a location of relatively strong signal along C.

Next at R_1 the sensors can be rotated around the x' axis until the z' axis is parallel to the z axis, and the y' axis is parallel to the y axis, by observing (using (6.4)) that

$$\begin{aligned} \tilde{X}_{z',z'}(s) &= \tilde{X}_{z,z}(s) \text{ contains only } \tilde{M}_z(s) \left(\text{no } \tilde{M}_t(s)\right) \\ \tilde{X}_{y',y'}(s) &= \tilde{X}_{y,y}(s) \text{ contains only } \tilde{M}_t(s) \left(\text{no } \tilde{M}_z(s)\right) \\ \vec{1}_R &= \vec{1}_y \\ \overleftrightarrow{X}(s) &= \frac{1}{16\pi^2 R^6}\left[\tilde{M}_t(s)\left[\vec{1}_x\vec{1}_x + 4\,\vec{1}_y\vec{1}_y\right] + \tilde{M}_z(s)\vec{1}_z\vec{1}_z\right] \end{aligned} \tag{6.18}$$

This results in the complete *physical* diagonalization of the signal dyadic (only three non zero components). Furthermore, this determines the orientation $\pm\vec{1}_z$ as can be seen from a z-oriented magnetic dipole at the target giving a magnetic field perpendicular to the target plane everywhere on this plane.

From R_1 move the sensors perpendicular to C in the sensor plane until R_0 is found (Case 1). From our knowledge of $\pm\vec{1}_z$ we know the direction to R_0. We can also correct for some measurement errors by noting that at P_0 $\tilde{N}(s)$ also has a null. From $\pm \overrightarrow{1}_z$ we have the target orientation, with P_0 we have a line through the target, and with P_1 (or merely the target plane containing C and perpendicular to $\pm \overrightarrow{1}_z$) we have $\overrightarrow{r}_0$, the target location.

In magnetostatic detection of buried ferrous targets, one can use gradiometer techniques to locate the target from its induced magnetic-dipole moment [11 (W. M. Wynn, Ch. 11)]. With symmetry, one can also use $\overleftrightarrow{\tilde{M}}(0)$ in (2.1) (for the case of ferrous targets) to extend the use of magnetostatics provided one has 3-axis magnetostatic illumination (using other than the earth's magnetostatic field). Utilizing the full description with the decomposition into longitudinal and transverse natural frequencies and modes gives yet more information for target identification as well as location and orientation.

7. Concluding Remarks

In order to apply this technique to the location and orientation of a buried rotational target (C_N for N ≥ 3), one needs to separate $\tilde{M}_z(s)$ and $\tilde{M}_t(s)$ in the target scattering. If one has identified the particular type of target (model of mine or UXO) from the natural frequencies (MSI sense), then one can use the fact that one set of the s_α (say $s^{(z)}{}_\alpha$) belongs to $\tilde{M}_z(s)$ and another set (say $s^{(t)}{}_\alpha$) belongs to $\tilde{M}_t(s)$. In the previous discussion the residues of these natural frequencies can be used in place of $\tilde{M}_z(s)$ and $\tilde{M}_t(s)$ to find the various nulls. So implementation of this technique may rely first on sufficiently accurate identification of the target and measurement of residues.

It is not necessary for the transmitted and receiver coils to be small compared to R provided they have sufficient symmetry (rotation and/or reflection) to align appropriate axes/planes with those of the target. Thereby one can increase the sensitivity of the measuring apparatus. Of course, away from these symmetry nulls the functional form of the response is more complicated than that in (6.1) if he coils are too large to be characterized by magnetic-dipole moments.

References

1. C. E. baum, Two-Dimensional Coils for Low-Frequency Magnetic Illumination and Detection, Sensor and Simulation Note 406, November 1996.

2. C. E. Baum, Low-frequency Near-Field magnetic Scattering from Highly, but Not Perfectly, Conducting Bodies, Interaction Note 499, November 1993.

3. C. E. Baum, The Magnetic Polarizability Dyadic and Point Symmetry, Interaction Note 502, May 1994.

4. C. E. Baum, Discrimination of Buried Targets Via the Singularity Expansion, Interaction Note 521, August 1966; Inverse Problems, Vol. 13, 1997, pp. 557-570.

5. C. E. Baum, Symmetry in Electromagnetic Scattering as a Target Discriminant, Interaction Note 523, October 1996; in H. Mott and W.-M. Boerner (eds.), Wideband Interferometric Sensing and Imaging Polarimetry, July 1977, Proc. SPIE, Vol. 3120, pp. 295-307.

6. C. E. Baum, Measures of Cross-Polarization for Discrimination of Symmetrical Targets, Interaction Note 538, March 1998.

7. I. J. Won et al, GEM-3: A Monostatic Broadband Electromagnetic Induction Sensor, J. Environmental & Engineering Geophysics, Vol. 2, March 1997, pp. 53-64.

8. L. Carin, R. Kapoor, and C. E. Baum, Polarimetric SAR Imaging of Buried landmines, IEEE Trans. Geoscience and Remote Sensing (in publication).

9. C. E. Baum, Electromagnetic Sensor and Measurement Techniques, pp. 73-144, in J. E. Thompson and L. H. Luessen, *Fast Electrical and Optical Measurements*, Martinus Nijhoff, Dordrecht, 1986.

10. C. E. Baum and H. N. Kritikos, Symmetry in Electromagnetics, Ch. 1, pp. 1-90, in C. E. Baum and H. N. Kritikos (eds.), *Electromagnetic Symmetry*, Taylor & Francis, 1995.

11. C. E. Baum (ed.), *Detection and Identification of Visually Obscured Targets*, Taylor & Francis (in publication).